Biochemical Characterization of the HIV-1 Integrase 3′-Processing Activity and Its Inhibition by Phosphorothioate Oligonucleotides†

Enzo Tramontano,‡ Paolo La Colla,*,‡ and Yung-Chi Cheng§

Dipartimento di Biologia Sperimentale, Università degli Studi di Cagliari, V.le Regina Margherita 45, 09100 Cagliari, Italy, and Department of Pharmacology, Yale University School of Medicine, 333 Cedar Street, New Haven, CT 06510

Received November 13, 1997; Revised Manuscript Received February 25, 1998

ABSTRACT: To better understand HIV-1 integrase (IN) functions, we determined the kinetic parameters of the 3′-processing reaction. Steady-state kinetic analysis performed using Dixon plots indicated that the concentration of active enzyme was 10-fold lower than that calculated by protein determination. The turnover number was low, suggesting that IN remained bound to DNA after cleavage. The catalytic efficiency increased 10-fold from 30 to 37 °C and 2-fold from 37 to 42 °C. In enzyme assays carried out at 37 °C, both single- and double-stranded phosphorothioate oligos bound to IN with an efficiency comparable to that of the phosphodiester duplex substrate. The competition efficiency of single-stranded oligos was directly related to the sequence length. On the other hand, phosphorothioate duplex U5 LTRs modified in the plus strand were capable of both competing with the substrate and directly inhibiting the 3′-processing activity. These results suggest that, in addition to other modes of action (inhibition of gp120-CD4 interaction and reverse transcriptase), phosphorothioate hetero- and homopolimeric oligos also potently inhibit the IN activity.

Integration of a double-stranded DNA copy of the viral genome into the DNA of a newly infected cell is an essential step in the HIV-1[1] life cycle (*1*−*3*). Integration is carried out by a virus-coded enzyme, the integrase (IN), which mediates recognition and binding of substrate DNAs and catalyzes coordinated reactions of processing and joining (*4*, *5*).

The 3′-processing reaction takes place in the cytoplasm (*6*) following reverse transcription of the viral RNA into a blunt-ended DNA. On the latter the enzyme recognizes specific sequences, which are present at both U5 and U3 termini of the viral long terminal repeats (LTR), and removes the last two nucleotides (GT) leaving recessed 3′-hydroxyl ends (*7*). The joining reaction takes place in the nucleus, where the preintegration complex binds to the host DNA (*8*). This step involves a nucleophilic attack (by the above 3′-hydroxyl ends) on phosphodiester bonds located 5 base pairs apart on either strand of the cellular DNA. The transesterification reaction produces an intermediate in which the 3′-ends of the viral DNA are covalently linked to the host DNA while the 5′-ends are flanked by 5 base pair gaps. Removal of mispaired nucleotides and gap repair, which are likely carried out by cellular enzymes, lead to completion of the integration process (*4*, *5*).

To define the mechanisms of retrovirus integration and to develop compounds targeted at IN, a number of in vitro assays have been described which employ recombinant IN and double-stranded oligodeoxynucleotide substrates that reproduce the viral U5 and/or U3 LTR termini (*9*−*18*). A comparison of these assays reveals that they differ not only in type of substrate and methods chosen to detect reaction products but also in experimental conditions such as temperature, which is known to affect enzyme kinetics and interaction with inhibitors. Moreover, kinetic parameters of the 3′-processing reaction have been determined according to Henry−Michaelis−Menten assumptions, although equimolar concentrations of enzyme and substrate (rather than an excess of substrate) have been used (*19*).

Therefore, with the aim to obtain more insights into the properties of the HIV-1 IN, we investigated the temperature dependence and determined the kinetic parameters of the 3′-processing reaction using Dixon plots (*20*). We performed these studies using a method (*11*) which allows a direct and accurate measure of the amount of substrate produced, coupled with the analysis of reaction products by denaturing PAGE.

Although the HIV-1 IN fails to process the 3′ ends of double-stranded DNA unrelated to its LTR termini, the IN-mediated processing of an LTR substrate can be inhibited by competition with LTR as well as non-LTR oligonucleotides (*21*). Since it has been reported that other HIV-1 processing enzymes, such as the reverse transcriptase, are

† This work was supported by Grant CA4435A and a Fellowship to E.T. from Istituto Superiore di Sanità.

* To whom correspondence should be addressed

‡ Università degli Studi di Cagliari.

§ Yale University School of Medicine.

[1] Abbreviations: AIDS, acquired immunodeficiency syndrome; CHAPS, (3-[(3-Cholamidopropyl) dimethylammonium]-1-propane-sulphonate); dC_n, phosphodiester polydeoxycytidine; DTT, dithiothreitol; EBV, Epstein-Barr virus; EDTA, ethylenediaminetetraacetic acid; HIV-1, human immunodeficiency virus type 1; IC_{50}, compound concentration required to inhibit enzyme activity by 50%; IN, integrase; IPTG, isopropyl β−D-thiogalactopyranoside; LTR, long terminal repeat; Oligo, oligonucleotide; MLV, murine leukemia virus; PAGE, polyacrylamide gel electrophoresis; PO, phosphodiester linkage; PS, phosphorothioate linkage; RSV, Rous sarcoma virus; S-dC_n, phosphorothioate polydeoxycytidine; RT, reverse transcriptase; SDS, sodium dodecyl sulfate.

S0006-2960(97)02792-X CCC: $15.00
Published on Web 05/02/1998

inhibited following interaction with backbone-modified hetero- and homopolymeric substrates (*22*), we evaluated whether phosphorothioate LTR substrates and dC_n oligos were able to inhibit the 3′-processing reaction.

EXPERIMENTAL PROCEDURES

Materials. The pINSD·His vector was kindly provided by Dr. R. Craigie (NIH). *Escherichia coli* BL21(DE3), His-bind resin, and purification kit were purchased from Novagen; IPTG and CHAPS, from Sigma; and HiTrap desalting columns and DEAE-Sephacel resin, from Pharmacia. Gel-purified phospodiester and phosphorothioate oligos were purchased from the DNA Synthesis Laboratory, Department of Pathology, Yale University. The Klenow polymerase, G-25 Sephadex quick spin columns, and dTTP were purchased from Boehringer Mannheim. [α-^{32}P]dGTP and [γ-^{32}P]ATP were purchased from Amersham. Multiscreen 96-well filtration plates (HV, 0.45 mm) were purchased from Millipore. T4-polynucleotide kinase was purchased from New England Biolabs.

Integrase Expression and Purification. Expression of the IN protein with an amino-terminal polyhistidine tag was accomplished by IPTG induction of the *E. coli* strain BL21-(DE3) containing the pINSD·His vector. Protein purification was carried out following the Novagen procedure, except for the presence of 5 mM CHAPS in the binding buffer (5 mM imidazole, 0.5 M NaCl, and 20 mM Tris-HCl, pH 7.9), the washing buffer (60 mM imidazole, 0.5 M NaCl, and 20 mM Tris-HCl, pH 7.9) and the elution buffer (1 M imidazole, 0.5 M NaCl, 50 mM Tris-HCl, pH 7.9 and 5 mM β-mercaptoethanol). Fractions were collected, and 3′-processing activity and protein concentration were determined. Protein purity was checked by SDS−PAGE and found to be higher than 90%. Imidazole, which was present in the elution buffer and, therefore, in the enzyme assays at a final concentration of 5−40 mM, was found to significantly increase IN activity (data not shown). Therefore, enzyme-containing fractions were pooled and loaded onto a HiTrap desalting column equilibrated in elution buffer without imidazole. Fractions were collected, and 3′-processing activity and protein concentration were determined. Enzyme-containing fractions were pooled, and aliquots were frozen at −80 °C.

Oligonucleotide Substrates. The following oligos representing the terminal 21 nucleotides of the HIV-1 U5 LTR were used in this study: **A**, 5′-GTG TGG AAA ATC TCT AGC AGT-3′ [plus strand]; **B**, 5′-ACT GCT AGA GAT TTT CCA CAC-3′ [minus strand]; and **C**, 5′ GTG TGG AAA ATC TCT AGC A −3′ [plus strand two nucleotides shorter than **A**]. For standard 3′-processing assays, **C** was annealed with **B** in 0.1 M NaCl by heating at 80 °C and slowly cooling to room temperature overnight. This double-stranded substrate was labeled by introducing at the 3′ end of **C** the two missing nucleotides using [α-^{32}P]dGTP, cold dTTP, and Klenow polymerase. Unincorporated [α-^{32}P]dGTP was separated from the duplex substrate by two consecutive runs through G-25 Sephadex quick spin columns. Alternatively, **A** was labeled at the 5′ end using [γ-^{32}P]ATP and T4 polynucleotide kinase, purified through a G-25 Sephadex quick spin column and then annealed with unlabeled **B** in 0.1 M NaCl as stated above.

A and **B** were also synthesized as phosphorothioate oligos.

3′-Processing Assays. Standard reaction conditions: 40 mM NaCl, 10 mM $MnCl_2$, 25 mM Tris-HCl, pH 7.5, 1 mM DTT, 2% glycerol, 1 nM duplex **B**:**C** labeled at the 3′ end, and 5 nM IN (considered as monomer). Unless otherwise stated, incubation was carried out at 37 °C for 30 min in a volume of 50 μL. The reaction was stopped by adding an equal volume of 0.5 M Na_2HPO_4. Each sample (90 μL) was added to a well of a Multiscreen 96-well filtration plate preloaded with 100 μL of DEAE-Sephacel slurry (equilibrated in 0.5 M Na_2HPO_4) which had been vacuum-dried. Vacuum was applied after incubation at room temperature for 10 min. The uncleaved, labeled substrate was retained in the resin, whereas labeled dinucleotide (GT) products were collected at the bottom of 96-well filtration plates and counted for radioactivity. When reactions were analyzed by denaturing PAGE, 6 μL of each sample was taken before the reaction was stopped, and this 6-μL aliquot was added to 3 μL of sample buffer (96% formamide, 20 mM EDTA, 0.08% bromophenol blue, and 0.25% xylene cyanol). Samples were heated at 100 °C for 3 min, layered onto a denaturing 15% polyacrylamide gel (7 M urea, 0.09 M Tris borate, pH 8.3, 2 mM EDTA, and 15% acrylamide) and run for 1 h at 65 W. Reaction products were visualized by autoradiography. Alternatively, 1 nM duplex **A**:**B** labeled at the 5′ end was used as substrate. In this case, 6 μL of each sample was added to 3 μL of sample buffer and run as described above.

Kinetic Constants. As described by Dixon (*19*, *20*), the kinetic constants were evaluated graphically by drawing a series of lines from the origin through points on the velocity curve where $v = [(n - 1)/n]V_{max}$, where n is a whole number and, thus, the points correspond to $^1/_2V_{max}$, $^1/_3V_{max}$, and so on. Each line intersects a horizontal line of height V_{max} at different points $[S]_n$. The distance between $[S]_2$ and $[S]_3$, $[S]_3$ and $[S]_4$, and so on, is the same and represents the K_m value.

The Dixon plot also allows one to verify whether a portion of the substrate is bound to the enzyme by drawing a line for $n = 1$, offset by an increment of K_m to the left of the $n = 2$ line. If the distance between the v axis and $[S]_1$ is greater than the K_m value, it is possible to conclude that a substantial portion of the total substrate is bound to the enzyme. Furthermore, the total enzyme concentration can be determined by drawing a similar line for $n = 0$. The distance between the v axis and $[S]_0$ indicates the $[E]_t$. The k_p values were expressed as the $V_{max}/[E]_t$ ratio.

Thermodynamic Parameters. The activation energy (E_a) was calculated by measuring the catalytic constants at different temperatures and plotting log k_p versus $(1/T)$ according to the Arrhenius equation (*23*).

RESULTS

Assay Conditions and Time Course of the 3′-Processing Reaction. In this study recombinant IN was incubated with a U5 LTR substrate which was labeled at the dinucleotide removed in the 3′-processing reaction. In the method originally described by Billich et al. (*11*), separation of the labeled reaction products was performed by adding to reaction mixtures a suspension of DEAE-Sephacel to bind the 21mer duplex substrate and to leave GT dimer products in the supernatant. Here, we used Multiscreen 96-well

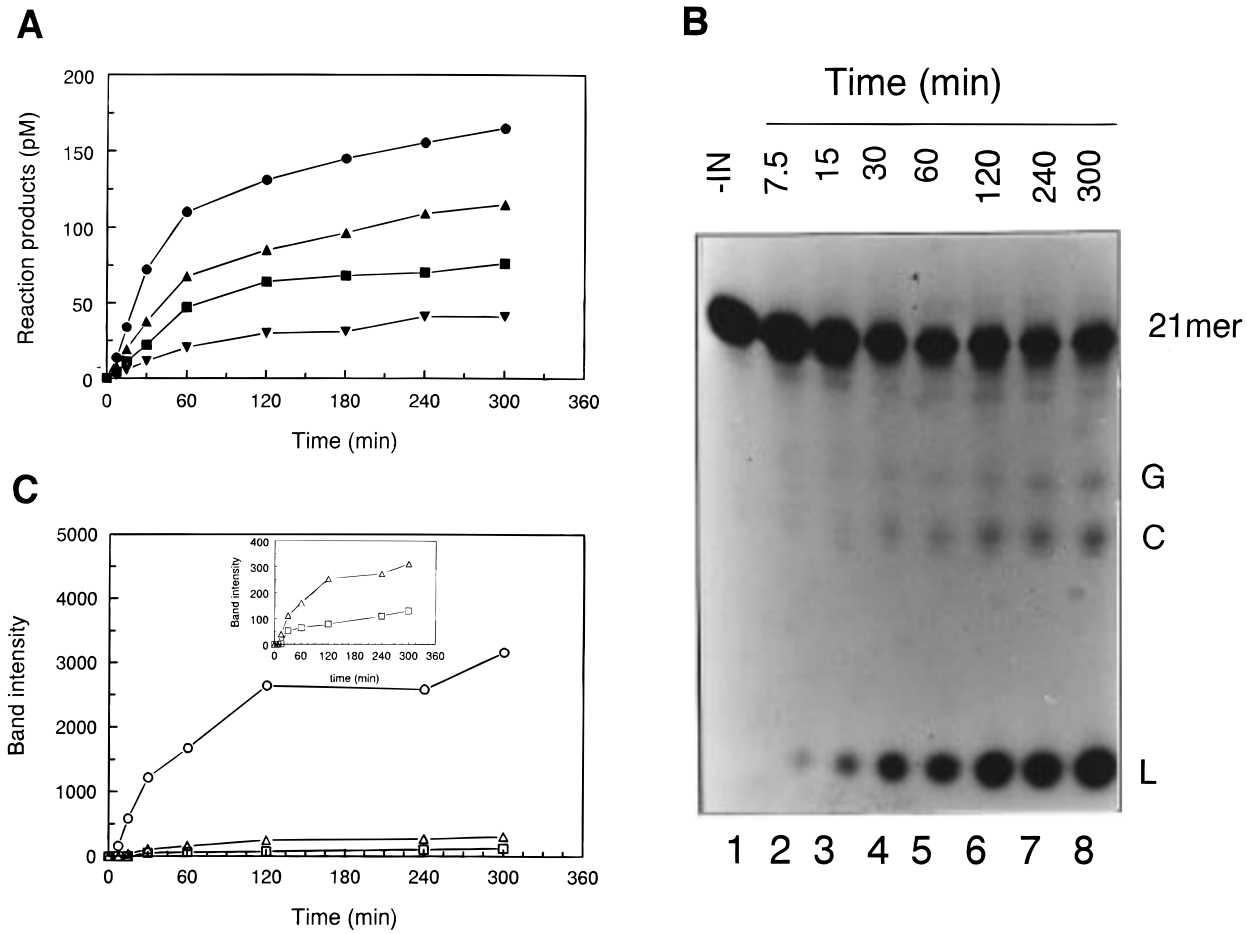

FIGURE 1: Time-course of the 3′-processing reaction. 3′-End-labeled 21mer duplex (1 nM) was incubated for the indicated times with HIV-1 IN at 37 °C. (A) IN concentration was 10 (●), 5 (▲), 2.5 (■), and 1.25 nM (▼). At the end of incubation, samples were processed in Multiscreen plates and filtrates were counted for radioactivity. (B) IN concentration was 10 nM. At the end of incubation, reaction products were analyzed by 15% PAGE and monitored by autoradiography. Lane 1, DNA alone; lanes 2−8, +IN. (C) Densitometric quantification of the bands G (□), C (△) and L (○) from the gel shown in panel B. The inset shows bands G and C plotted on a different scale.

filtration plates preloaded with DEAE-Sephacel, so that the labeled GT dimers could be collected at the bottom of the plates. This allowed a measure of the 3′-processing activity more rapid and accurate than PAGE.

Following optimization of NaCl, $MnCl_2$, and glycerol concentrations, which turned out to be 40 mM, 10 mM and 2%, respectively, the time course and the temperature dependence of the 3′-processing reaction were determined by both Multiscreen assay and PAGE.

Time course studies (Figure 1A), performed at 37 °C with 1 nM substrate and IN concentrations ranging from 1.25 to 10 nM, revealed that the reaction was linear up to 30 min and plateaued after 1 h. As expected, when analyzed by denaturing PAGE (Figure 1B), three reaction products were observed depending on the nucleophile group that attacked the phosphodiester linkage. From top to bottom they were the glycerol adduct (G), the cyclic dinucleotide (C), and the linear dinucleotide (L), which formed following the attack of glycerol, the 3′-OH end of the substrate, and water, respectively (*14*). Quantitation of band intensity (Figure 1C) revealed that formation of the three reaction products had time courses similar to those shown in Figure 1A, and that the L form accounted for approximately 80% of the reaction products.

When reaction rates were plotted against enzyme concentrations, linear relationships were obtained (data not shown), suggesting that the processing rate was first-order with respect to IN and that, although the enzyme was present in amounts higher than substrate, its concentration was the rate-limiting step.

Determination of Kinetic Constants. The latter observations suggested that the concentration of active IN was significantly lower than that nominally added, as calculated (for a monomeric form of the enzyme) on the basis of protein determination. However, it was still possible that concentrations of IN and substrate were in the same order of magnitude. Therefore, due to the fact that a significant fraction of the 21mer duplex was likely bound to the enzyme, the Henry−Michaelis−Menten equations were inadequate to determine steady-state kinetic parameters. We thus used the more general method described by Dixon (*19*, *20*) and found (Figure 2) that V_{max} and K_m values at 37 °C were 6.8 pM h^{-1} and 0.15 nM, respectively. Furthermore, the distance between the v axis and the intercept between the $n = 1$ and V_{max} lines was greater than the K_m value (Figure 2), demonstrating that a substantial portion of the substrate was bound to the enzyme. Moreover, since the distance between the v axis and the intercept between the $n = 0$ and V_{max} lines

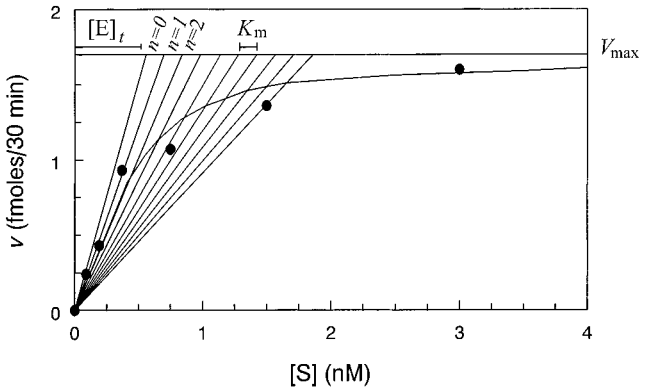

FIGURE 2: Steady-state kinetics of the 3′-processing reaction at 37 °C. 3′-End-labeled 21mer duplex (1 nM) was incubated for 30 min with HIV-1 IN (5 nM) at 37 °C. Samples were processed in Multiscreen plates, and filtrates were counted for radioactivity. The plot indicates the V_{max} line, the line drawn for $n = 2$, the K_m increment, and the distance between the v axis and the $n = 0$ line.

Table 1: Steady-State Parameters of the 3′-Processing Reaction at Different Temperatures[a]

temperature (°C)	K_m (nM)	k_p[b] (h^{-1})	k_p/K_m (h^{-1}/nM^{-1})
30	0.42	0.037	0.088
37	0.15	0.126	0.840
42	0.15	0.231	1.540

[a] 3′-End-labeled 21mer duplex (1 nM) was incubated for 30 min with 5 nM IN at 42 or 37 °C and with 10 nM IN at 30 °C. Samples were processed in Multiscreen plates and counted for radioactivity.[b] k_p values were calculated from the ratio V_{max}/[IN], where [IN] was obtained from kinetic analysis.

gave an $[E]_t$ value of 0.54 nM, the concentration of *active* enzyme resulted to be one-tenth of that added to each assay, as calculated on the basis of protein determination.

The turnover number (k_p value) calculated at 37 °C using this enzyme concentration was 0.126 h^{-1} (Table 1).

Temperature Dependence and Thermodynamic Parameters. Time courses of the 3′-processing reaction at 30, 37, and 42 °C showed that, in addition to the length of incubation, the temperature also influenced the reaction rate and the amount of products at plateau, which were at a minimum at 30 °C and a maximum at 42 °C (Figure 3A). Nevertheless, PAGE analysis of reaction products (Figure 3B) showed that 3′-processing resulted in the usual major products G, C, and L, no matter which reaction temperature was used, indicating that the temperature had no influence on the type of nucleophile attack on the phosphodiester linkage. When the rates of the reactions performed at 30 and 42 °C were plotted against enzyme concentrations (data not shown), linear relationships were obtained comparable to those found at 37 °C. Again, Dixon kinetic plots (data not shown) allowed us to conclude that a significant portion of the substrate was bound to the enzyme also at 30 and 42 °C, and that the concentration of active IN was about 10-fold lower than that calculated on the basis of protein determination.

When 3′-processing assays were carried out at 30 and 42 °C, K_m values of 0.42 and 0.15 nM and k_p values of 0.037 and 0.231 h^{-1} were found, respectively (Table 1). The possibility that the above difference in k_p values could be due to temperature-related changes in enzyme conformation was examined by drawing a plot of log k_p versus $1/T$ (Figure 3C). However, the linearity of the plot indicated that no change in enzyme conformation occurred. The activation energy (E_a) calculated was 28.1 kcal/mol. Furthermore, the plot of log k_p/T versus $1/T$ was also linear, and the ΔH calculated was 27.5 kcal/mol (data not shown).

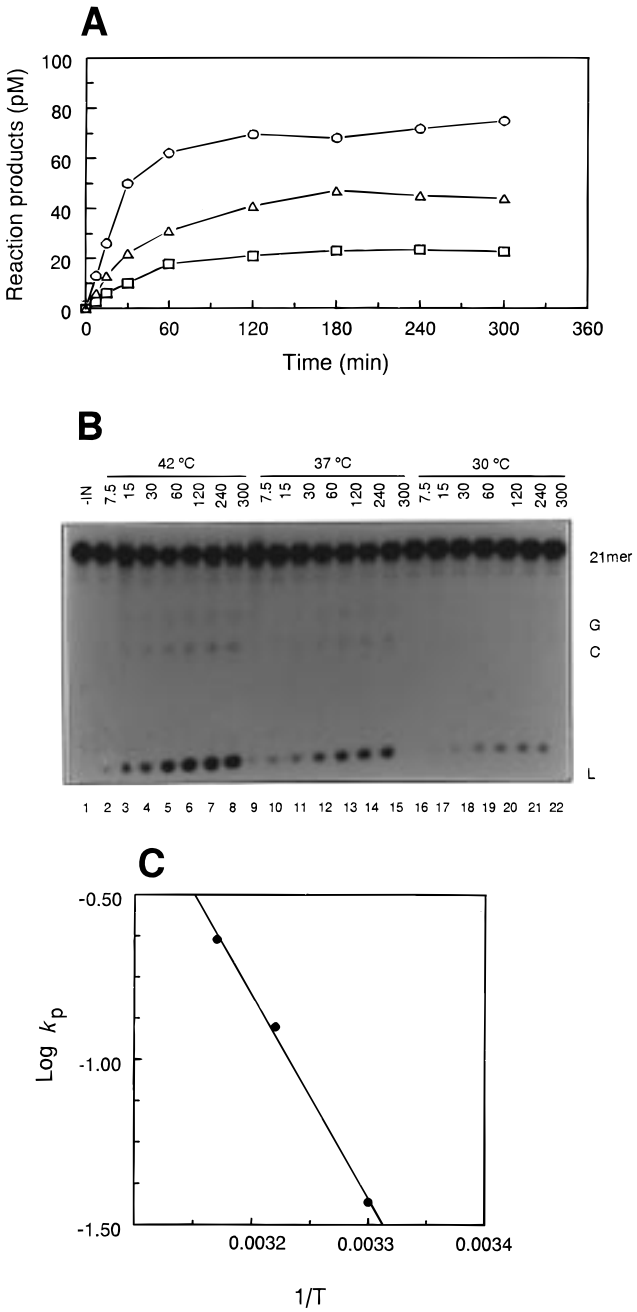

FIGURE 3: Time-course of the 3′-processing reaction at different temperatures and determination of thermodynamic parameters. (A) 3′-end-labeled 21mer duplex (1 nM) was incubated for 30 min with 5 nM HIV-1 IN at 42 (○) or 37 °C (△) and with 10 nM IN at 30 °C (□). Samples were processed in Multiscreen plates, and filtrates were counted for radioactivity. (B) Reaction products were analyzed by 15% PAGE and monitored by autoradiography. Lane 1, DNA alone; lanes 2−8, 9−15, and 16−22, +IN and incubation at 42, 37, and 30 °C, respectively. (C) Arrhenius plot drawn for E_a determination.

3′-Processing Inhibition by Phosphorothioate Oligos. DNA substrates carrying phosphorothioate or methylphosphonate substitutions at the site of cleavage, or 5′ or 3′ to the latter, have been used to investigate the mechanism of

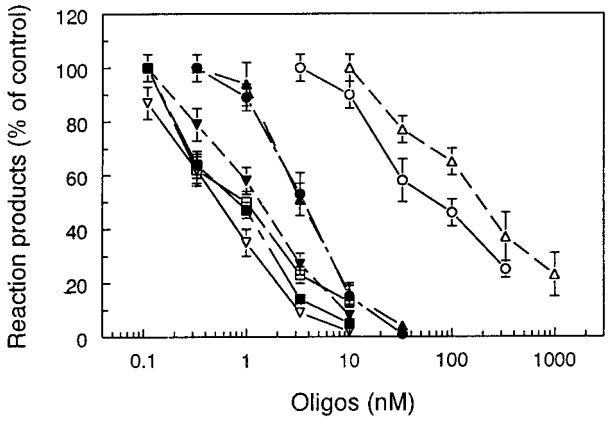

FIGURE 4: Competition of the 3′-processing activity with single- and double-stranded phosphodiester and phosphorothioate U5 LTR oligos. 3′-End-labeled 21mer duplex (1 nM) was incubated for 30 min at 37 °C with HIV-1 IN (5 nM), alone or in the presence of increasing amounts (0.1−3000 nM) of unlabeled oligos $\mathbf{A}_{PO}$ (○), $\mathbf{B}_{PO}$ (△), $\mathbf{A}_{PS}$ (●), $\mathbf{B}_{PS}$ (▲), $\mathbf{A}_{PO}$:$\mathbf{B}_{PO}$ (□), $\mathbf{A}_{PO}$:$\mathbf{B}_{PS}$ (■), $\mathbf{A}_{PS}$:$\mathbf{B}_{PO}$ (▽), and $\mathbf{A}_{PS}$:$\mathbf{B}_{PS}$ (▼). Samples were processed in Multiscreen plates, and filtrates were counted for radioactivity.

the different IN activities (*8*, *24*). We extended these studies by investigating whether phosphorothioate oligos, which are known to selectively inhibit the HIV-1 multiplication with non-sequence-specific mechanisms, were also potent inhibitors of the 3′-processing reaction.

In a first series of experiments, IN was incubated with a 3′-end-labeled 21mer substrate in the presence of each of the following unlabeled U5 LTR oligos as competitors: phosphodiester (PO) or phosphorothioate (PS) single-stranded plus (**A**) and minus (**B**) 21mer sequences, and the duplexes resulting from their combinations. The aim was to investigate whether phosphorothioate oligos had a greater affinity for IN than native substrates. Dose−response curves illustrating competition of the 3′-processing reaction (Figure 4) showed that phosphodiester single-stranded plus and minus U5 LTR strands were poor competitors, whereas backbone modification with thioate residues increased their competition efficiency by 27- and 62-fold, respectively. Vice versa, phosphorothioate double-stranded oligos were competitors as efficient as phosphodiester substrates, independently of which strand (plus, minus, or both) carried the backbone modification. This suggested that phosphorothioate single- and double-stranded U5 LTR sequences bound to IN with the same efficiency as the phosphodiester duplex substrate, and that such an interaction precluded binding and sequence-dependent cleavage of the LTR termini by the enzyme.

Then, we investigated whether phosphorothioate U5 LTR oligos could be used as substrates in the 3′-processing reaction. To this end, the formation of 19mer products from the four different 5′-end-labeled 21mer duplex substrates (Figure 5) was analyzed by PAGE. When the phosphorothioate linkages were present only on the minus DNA strand (which is not subjected to 3′-processing), the HIV-1 IN used as substrate the oligo $\mathbf{A}_{PO}$:$\mathbf{B}_{PS}$ as efficiently as the phosphodiester duplex $\mathbf{A}_{PO}$:$\mathbf{B}_{PO}$. On the contrary, when the phosphorothioate linkages were on the plus strand (see $\mathbf{A}_{PS}$:$\mathbf{B}_{PO}$ and $\mathbf{A}_{PS}$:$\mathbf{B}_{PS}$), the enzyme could not perform the 3′-processing reaction.

Since thioate residues were capable of converting single-stranded (plus and minus) U5 LTR sequences into competitors as efficient as the U5 LTR duplex substrate, it was interesting to evaluate whether this held true also for single-stranded homopolymers such as polydeoxycytidines and whether their length had any influence on the competition efficiency (Table 2). When phosphodiester polydeoxycytidines (dC_n) were added to standard reaction mixtures, the potency in reducing the 3′-processing reaction and the length of the homopolymers were directly related. Phosphorothioate polydeoxycytidines (S-dC_n) were more efficient inhibitors than phosphodiester counterparts of corresponding length, and also in this case, inhibitory potency and length of the oligos were directly related.

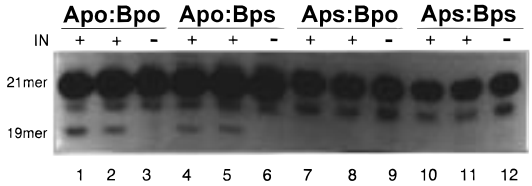

FIGURE 5: 3′-Processing of phosphorothioate substrates. 5′-End-labeled oligos $\mathbf{A}_{PO}$ and $\mathbf{A}_{PS}$ were annealed with oligo $\mathbf{B}_{PO}$ or $\mathbf{B}_{PS}$ and used as substrates (1 nM) in an enzyme assay with HIV-1 IN (5 nM) at 37 °C for 30 min. The labeled 19mer reaction products were separated by 15% PAGE and monitored by autoradiography. Lanes 3, 6, 9, and 12, DNA alone. Lanes 1 and 2, 4 and 5, 7 and 8, and 10 and 11, duplicate samples +IN with indicated duplex substrates.

Table 2: Inhibition of the 3′-Processing Reaction by Phosphodiester and Phosphothioate Polydeoxycytidines[a]

oligonucleotide	IC_{50}[b] (nM)	oligonucleotide	IC_{50}[b] (nM)
dC_{11}	> 3000	S-dC_{11}	39 ± 10
dC_{14}	610 ± 90	S-dC_{14}	6.3 ± 0.3
dC_{18}	90 ± 9	S-dC_{18}	4.2 ± 0.8
dC_{21}	52 ± 7	S-dC_{21}	1.5 ± 0.5
dC_{28}	10 ± 2	S-dC_{28}	1.8 ± 0.1

[a] 3′-End-labeled 21mer duplex (1 nM) was incubated for 30 min with 5 nM IN at 37 °C. Samples were processed in Multiscreen plates and counted for radioactivity. [b] Compound concentration required to reduce processing of 3′-end-labeled 21mer substrate by 50%. Data represent mean values ± SD from three independent determinations.

DISCUSSION

The present study describes kinetic studies of the 3′-processing by HIV-1 integrase and the inhibition of this process by phosphorothioate oligonucleotides.

Like previous studies, our 3′-processing assays were carried out with a nominal excess of enzyme (5 nM) over substrate (1 nM). Therefore, since the derivation of the Henry−Michaelis−Menten equation assumes that the total substrate concentration $[S]_t$ is much greater than the total enzyme concentration $[E]_t$, we deemed more valid to perform steady-state kinetic analyses by Dixon plots, which are based on a simple velocity curve (*19*, *20*). As a result, we found that the enzyme concentration is about 10-fold lower than that estimated through protein determination. However, a possible explanation for this discrepancy is that, while kinetic studies allow one to calculate the concentration of active enzyme, which in this case is known to be a multimeric form of the protein (*25*−*27*), the assays for protein determination neither discriminate between active and inactive enzyme molecules nor reveal other phenomena such as poor enzyme solubility, protein multimerization, etc.

The low turnover number ($k_p = 0.126\ h^{-1}$) obtained at 37 °C is close to that ($k_p = 0.24\ h^{-1}$) obtained in the only other kinetic study (*16*) of which we are aware, and supports the hypothesis that, at the end of the 3′-processing reaction, the HIV-1 IN remains bound to the viral DNA. This result is consistent with the following observations: (i) the active site for both 3′-processing and strand transfer reactions is the same; (ii) the 3′-processing takes place in the cytoplasm, and the enzyme−viral DNA complex has to migrate to the nucleus, where the strand transfer reaction occurs; (iii) there is no need for the HIV-1 IN to turn over after 3′-processing, since only one copy of the viral DNA is integrated into the host DNA.

Although our kinetic data are also comparable to those reported for the MLV enzyme (*28*), which is unable to turn over, they differ from those obtained with the RSV IN ($k_p = 0.52\ min^{-1}$), which turns over efficiently (*25*). However, it cannot be excluded that the above differences among retroviral integrases may be due to differences in multimeric status, inactivation level, or solubility in low-salt buffers.

Steady-state kinetic studies performed at different temperatures showed that the catalytic efficiency of IN increases 10-fold when the incubation temperature is increased from 30 to 37 °C and 2-fold when the temperature is increased from 37 to 42 °C. Interestingly, the above phenomenon is due neither to changes in the enzyme conformation nor to enzyme inactivation. Moreover, variations in the incubation temperature do not alter the choice of the nucleophile groups which attack the phosphodiester linkage. Vice versa, the incubation temperature influences the kinetic energy and, therefore, the fruitful collision frequency and the enzyme−substrate dissociation, two factors which are probably responsible for the k_p increase as the temperature increases.

Previous studies have shown that phosphorothioate oligos inhibit selectively, although in a non-sequence-specific manner, the HIV-1 replication. Interference with the gp120-CD4 interaction (*29*) and competition with template−primer for the reverse transcriptase (*30*) have been claimed as possible modes of action. In this study, we produce evidence indicating that, in enzyme assays, phosphorothioate oligos are very potent inhibitors of the HIV-1 IN.

It is worth noting that, since the enzyme affinity for its substrate is higher at 37 than at 30 °C and the temperature-dependent change in energy may alter the IN−substrate/inhibitor interactions, we chose to perform these studies at 37 °C. Under these conditions, both single- and double-stranded phosphorothioate oligos bind to IN with efficiencies comparable to that of the phosphodiester duplex substrate; moreover, this interaction precludes binding and sequence-dependent 3′-processing of the LTR termini. In the case of single-stranded oligos, the competition efficiency and sequence length are directly related, as has been observed in enzyme assays with HIV-1 RT (*31*) and EBV DNA polymerase (*32*). In the case of double-stranded oligos reproducing the terminal 21 nucleotides of the HIV-1 U5 LTR sequence, phosphorothioate modification of the plus strand makes it capable not only to compete with the substrate but also to inhibit the 3′-processing activity. This result is particularly interesting due to the fact that the HIV-1 IN is able to efficiently process a double-stranded oligo carrying a phosphorothioate linkage between the purine nucleotides of the ···CAGT-3′ sequence (*8*).

Contrary to double-stranded counterparts, phosphorothioate single-stranded oligos are more potent inhibitors than phosphodiester oligos of equal length. The reason may be related to the negative charge delocalization on the phosphorothioate backbone or to the greater van der Waals attractive potential of sulfur which may determine a tighter interaction between the oligos and the enzyme.

Among phosphorotioate oligos, SdC_{28} has been one of the most extensively studied. Therefore, numerous data are available on its anti-HIV-1 activity, both in cell-based and enzyme assays, which allow a comparison of its inhibitory potency against putative targets: gp120-CD4 interaction, RT, and IN. SdC_{28} competes the binding of a modified oligonucleotide to a recombinant CD4 with a K_I value of 3.1 nM (*33*) and competitively inhibits the activity of the HIV-1 RT with a K_I value of 2.8 nM (*30*). In this study we show that SdC_{28} inhibits the 3′-processing activity of HIV-1 IN with an IC_{50} value of 1.8 nM, and since the Cheng−Prusoff equation allows us to calculate the K_I value of an inhibitor if K_m and IC_{50} values are known (*34*), SdC_{28} competes the IN substrate with a K_I value of 0.2 nM. Therefore, considering that in MT-4 cells acutely infected at low multiplicity of infection SdC_{28} inhibits the spreading of the HIV-1 infection with an EC_{50} of 30 nM (*35*), and it prevents the formation of syncytia between chronically infected MOLT 3 and uninfected CEM cells at 600 nM (*29*), integration of HIV-1 may well be a primary target of phosphorothioate hetero- and homopolimeric oligos.

ACKNOWLEDGMENT

We thank R. Craigie for providing us the pINSD·His vector through the NIH AIDS research and reference reagent program.

REFERENCES

1. LaFemina, R. L., Schneider, C. L., Robbins, H. L., Callahan, P. L., LeGrow, K., Roth, E., Schleif, W. A., and Emini, E. A. (1992) *J. Virol. 66*, 7414−7419.
2. Sakai, H., Kawamura, M., Sakuragi, J.-I., Sakuragi, S., Shibata, R., Ishimoto, A., Ono, N., Ueda, S., and Adachi, A. (1993) *J. Virol. 67*, 1169−1174.
3. Engelman, A., Englud, G., Orenstein, J. M., Martin, M. A., and Craigie, R. (1995) *J. Virol. 69*, 2729−2736.
4. Kulkosky, J., and Skalka, A. M. (1994) *Pharmacol. Ther. 61*, 185−203.
5. Andrake, M. D., and Skalka, A. M. (1996) *J. Biol. Chem. 271*, 19633−19636.
6. Roth, M. J., Schwartzberg, P. L., and Goff, S. P. (1989) *Cell 58*, 47−54.
7. Pauza, C. (1990) *Virology 179*, 886−889.
8. Engelman, A., Mizuuchi, K., and Craigie, R. (1991) *Cell 67*, 1211−1221.
9. Craigie, R., Mizuuchi, K., Bushman, F. D., and Engelman, A. (1991) *Nucleic Acids Res. 19*, 2729−2734.
10. Fitzgerald, M. L., Vora, A. C., and Grandgenett, D. P. (1991) *Anal. Biochem. 196*, 19−23.
11. Billich, A., Schauer, M., Frank., S., Rosenwirth, B., and Billich, S. (1992) *Antiviral Chem. Chemother. 3*, 113−119.
12. Carteau, S., Mouscadet, J. F., Goulaouic, H., Subra, F., and Auclair, C. (1993) *Arch. Biochem. Biophys. 300*, 756−760.
13. Fesen, M. R., Kohn, K. W., Leteurtre, F., and Pommier, Y. (1993) *Proc. Natl. Acad. Sci. U.S.A. 90*, 2399−2403.
14. Hazuda, D. J., Hastings, J. C., Wolfe, A. L., and Emini, E. A. (1994) *Nucleic Acids Res. 6*, 1121−1122.
15. Vink, C., Banks, M., Bethell, R., and Plasterk, R. H. A. (1994) *Nucleic Acids Res. 22*, 2176−2177.

16. Lee, S. P., Kim, H. G., Censullo, M. L., and Han, M. K. (1995) *Biochemistry 34*, 10205−10214.
17. Farnet, C. M., Wang, B., Lipford, J. R., and Bushman, F. D. (1996) *Proc. Natl. Acad. Sci. U.S.A. 93*, 9742−9747.
18. Robinson, W. E., Reinecke, M. G., Abdel-Malek, S., Jia, Q., and Chow, S. A. (1996) *Proc. Natl. Acad. Sci. U.S.A. 96*, 6326−6331.
19. Segel, I. H. (1975) *Enzyme kinetics*, pp 18−80, John Wiley & Sons, New York.
20. Dixon, M. (1972) *Biochem. J. 129*, 197−215.
21. LaFemina, R., Callahan, P. L., and Cordingley, M. G. (1991) *J. Virol. 65*, 5624−5630.
22. Stein, C. A., and Cheng, Y.−C. (1993) *Science 261*, 1004−1012.
23. Segel, I. H. (1975) *Enzyme kinetics*, pp 926−942, John Wiley & Sons, New York.
24. Mazumder, A., Gupta, M., and Pommier, Y. (1994) *Nucleic Acids Res. 22*, 4441−4448.
25. Jones, K. S., Coleman, J., Merkel, G. W., Laue, T. M., and Skalka, A. M. (1992) *J. Biol. Chem. 267*, 16037−16040.
26. Engelman, A., Bushman, F. D., and Craigie, R. (1993) *EMBO J. 12*, 3269−3275.
27. Ellison, V., Gerton, J., Vincent, K. A., and Brown, P. O. (1995) *J. Biol. Chem. 270*, 3320−3326.
28. Dotan, I., Scottoline, B. P., Heuer, T. S., and Brown, P. O. (1995) *J. Virol. 69*, 456−468.
29. Stein, C. A., Neckers, L. M., Nair, B. C., Mumbauer, S., Hoke, G., and Pal, R. (1991) *J. Acquired Immune Defic. Syndr. 4*, 686−693.
30. Majumdar, C., Stein, C. A., Cohen, J. S., Broder, S., and Wilson, S. H. (1989) *Biochemistry 28*, 1340−1346.
31. Marshall, W. S., Beaton, G., Stein, C. A., Matsukura, M., and Caruthers, M. H. (1992) *Proc. Natl. Acad. Sci. U.S.A. 89*, 6265−6269.
32. Gao, W., Stein, C. A., Cohen, J. S., Dutschman, G. E., and Cheng, Y.−C. (1989) *J. Biol. Chem. 264*, 11521−11526.
33. Yakubov, L., Khaled, Z., Zhang, L.-M., Truneh, A., Vlassov, V., and Stein C. A. (1993) *J. Biol. Chem. 268*, 18818−18823.
34. Cheng, Y.-C., and Prusoff, W. (1973) *Biochem. Pharmacol. 22*, 3099−3108.
35. Chou, T.-C., Zhu, Q.-Y., and Stein C. A. (1991) *AIDS Res. Hum. Retroviruses 7*, 943−951.
36. Stein, C. A., Neckers, L. M., Nair, B. C., Mumbauer, S., Hoke, G., and Pal, R. (1991) *J. Acquired Immune Defic. Syndr. 4*, 686−693.

BI972792O